

## Electronic Supporting Information (ESI)

### Tracking endoplasmic reticulum viscosity during ferroptosis and autophagy using molecular rotor probe

Akshay Silswal<sup>a</sup> and Apurba Lal Koner<sup>\*a</sup>

*<sup>a</sup>Bionanotechnology Lab, Department of Chemistry Indian Institute of Science Education and Research Bhopal, Bhopal Bypass Road, Bhauri, Bhopal-462066, Madhya Pradesh, INDIA, E-mail: [akoner@iiserb.ac.in](mailto:akoner@iiserb.ac.in)*

### Table of Content

Experimental Section	
Materials and Methods.....	2
Cell culture and imaging.....	2-3
Synthesis of compound <b>JER</b> .....	3-4
<b>Fig. S1:</b> <sup>1</sup> H NMR of compound <b>JER</b> .....	4
<b>Fig. S2:</b> HRMS of compound <b>JER</b> .....	5
<b>Fig. S3:</b> Absorption, emission and excitation spectra of <b>JER</b> .....	5
<b>Fig. S4:</b> Solvent dependent UV-Vis. and fluorescence spectra.....	6
<b>Table S1:</b> Solvent-dependent photophysical parameters of <b>JER</b> .....	6
<b>Fig. S5:</b> Steady-state fluorescence emission spectra of <b>JER</b> in different methanol glycerol mixture.....	7
<b>Fig. S6:</b> pH tolerance plot of the dye.....	7
<b>Fig. S7:</b> Photostability plot of the dye.....	8
<b>Fig. S8-9:</b> MTT assay of <b>JER</b> .....	8-9
<b>Fig. S10-11:</b> Cellular uptake of structurally similar <b>JER</b> derivative.....	9-10
<b>Fig. S12-16:</b> Colocalization experiment of <b>JER</b> in different cell lines.....	10-12
<b>Fig. S17-18:</b> Photostability plot of the dye under live cell conditions.....	13
<b>Fig. S19-20:</b> Control experiments for ferroptosis and ER-phagy.....	14
<b>Table S2</b> Reported viscosity sensitive probes for endoplasmic viscosity.....	15
References.....	15

## Experimental Section

### Materials and Methods:

All reagents and solvents were purchased from commercial sources and used without further purification. The neutral alumina was purchased from Rankem used for column chromatography.  $^1\text{H}$  and  $^{13}\text{C}$  NMR spectra were recorded on Bruker 500 MHz spectrometers. High-resolution mass spectrometry (HRMS) data were recorded on MicroTOF-Q-II mass spectrometer using methanol as the solvent. All absorption spectra and fluorescence measurements were carried out using SHIMADZU UV-1800 spectrophotometer and HORIBA JobinYvon fluorimeter (fluorolog-3) using 1 cm path length quartz cuvettes.

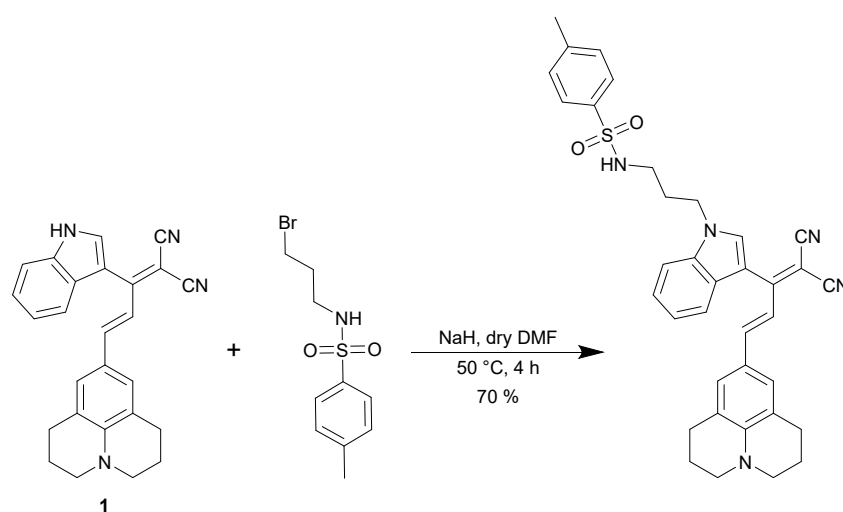
**Cell culture and imaging:** Dulbecco's Modified Eagle Medium (DMEM), Trypsin, Antibiotic cocktail and Fetal Bovine Serum (FBS) were purchased from HiMedia (USA). Lyso-Tracker Green, ER Tracker Green and MitoTracker Green were purchased from Thermo Fisher SCIENTIFIC (USA). The 35 mm glass bottom imaging dishes were obtained from Ibidi (Germany, Cat# S28 81158). All the confocal microscopy imaging was performed with an Olympus FV3000 Confocal Laser Scanning Microscope (LSM). Fluorescence lifetime imaging (FLIM) experiments were performed using confocal setup of PicoQuant, MicroTime 200 with an inverted optical microscope (Olympus IX-71) and analyzed by SymPhoTime 64 software. A549, R1610 and U-87 MG cells were obtained from NCCS, Pune, India and were grown in a 25 cm<sup>2</sup> cell culture flask (Corning, USA) using DMEM containing 10% (v/v) FBS and 1% (v/v) antibiotic cocktail in 5% CO<sub>2</sub> at 37 °C in a CO<sub>2</sub> incubator. For imaging purpose, cells were grown to 75% - 80% confluency in the 35 mm glass bottom imaging dishes ( $170 \pm 5 \mu\text{m}$ ) in DMEM with 10% FBS. For staining the cells 1 mM stock solution of **JER** was prepared in DMSO and further diluted to 1  $\mu\text{M}$  in PBS, the final concentration of DMSO in solution was 0.1 %. For colocalization experiment the cells were co-incubated with 1  $\mu\text{M}$  of the **JER**, and 300 nM of commercially available trackers for 30 minutes and washed with PBS (pH 7.4) twice before imaging.

For ferroptosis induction, firstly A549 cells were incubated with 10  $\mu\text{M}$  erastin for the indicated time period and then treated with 1  $\mu\text{M}$  **JER** for 30 mins and washed twice with PBS (pH 7.4) and immediately observed on confocal microscope. For the ferroptosis induction inhibitor experiment cells were incubated with 10  $\mu\text{M}$  erastin and 20  $\mu\text{M}$  ferrostatin-1 for the indicated time period and then treated with 1  $\mu\text{M}$  **JER** for 30 mins and washed twice with PBS (pH 7.4) and observed on confocal microscope. For FLIM analysis, A549 cells were incubated with 10

$\mu\text{M}$  erastin for 4 h and then treated with 1  $\mu\text{M}$  **JER** for 30 mins and washed twice with PBS (pH 7.4) and observed on the confocal microscope. For control, cells were treated with 1  $\mu\text{M}$  **JER** for 30 mins and imaged under the microscope after washing twice with PBS (pH 7.4). For ER-phagy experiment cells were treated with 300 nM LysoTracker Green and 1  $\mu\text{M}$  **JER** for 30 mins and washed then nutrient free media was added to it for the indicated time period and observed in the microscope.

### Synthetic Scheme:

Synthesis and characterization of Compound **1** is previously reported.<sup>1</sup>



### Synthetic Procedure:

Sodium hydride (6.75 mg, 0.28 mmol, 60% in oil) was washed with hexane and the compound **1** (100 mg, 0.26 mmol) kept in vacuum and then dry DMF (3 mL) was added to it dropwise and stirred for 30 mins at room temperature under  $\text{N}_2$  atmosphere. Then N-(3-bromopropyl)-4-methylbenzenesulphonamide (224 mg, 0.77 mmol) dissolved in DMF was added dropwise to reaction mixture and kept on stirring for 4 h at 50 °C. After completion, reaction mixture was dissolved in ice cold water and compound is extracted using ethyl acetate (3 x 20 mL). Combine organic phase was washed with brine and dried over anhydrous sodium sulphate. Then ethyl acetate was evaporated and product is collected. The blood red solid product was purified using column chromatography with neutral alumina gel and 20 % ethyl acetate/hexane and 1% triethyl amine as eluent with 70% yield.

$^1\text{H}$  NMR (500 MHz,  $\text{CD}_2\text{Cl}_2$ )  $\delta$  7.71 (d,  $J = 8.2$  Hz, 2H), 7.61 (s, 1H), 7.54 (d,  $J = 8.1$  Hz, 1H), 7.45 (d,  $J = 8.4$  Hz, 1H), 7.38 – 7.29 (m, 4H), 7.20 (t,  $J = 7.6$  Hz, 1H), 7.11 (d,  $J = 15.0$  Hz, 1H), 7.03 (s, 2H), 4.96 (t, 1H), 4.41 (t,  $J = 6.5$  Hz, 2H), 3.32 (t,  $J = 5.8$  Hz, 4H), 2.82 (q,  $J =$

6.0 Hz, 2H), 2.73 (t,  $J = 6.3$  Hz, 4H), 2.44 (s, 3H), 2.16 (q,  $J = 6.6$  Hz, 2H), 2.01 – 1.92 (m, 4H).

ESI HRMS  $m/z$   $[M+ Na]^+$  calculated mass = 624.2404 Da, obtained mass = 624.2407 Da

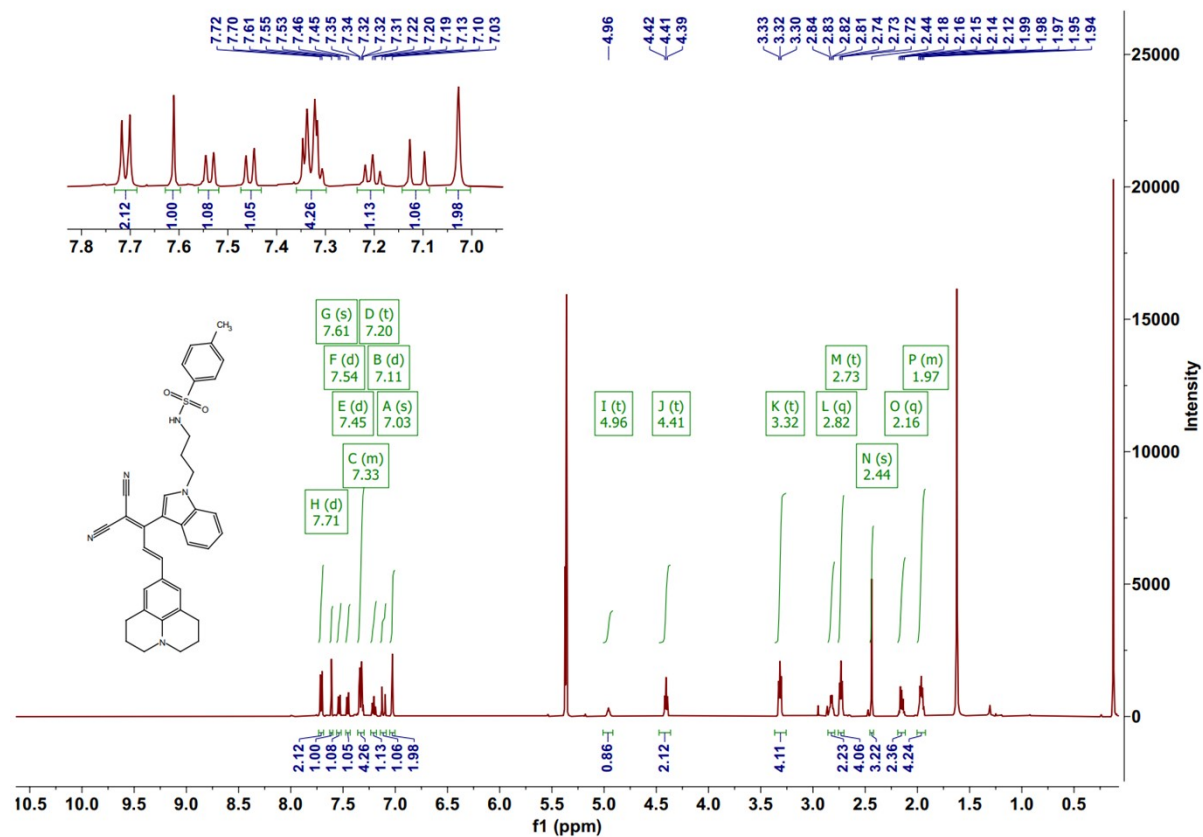


**Fig. S1**  $^1\text{H}$  NMR spectrum of JER in  $\text{CD}_2\text{Cl}_2$  recorded at 500 MHz

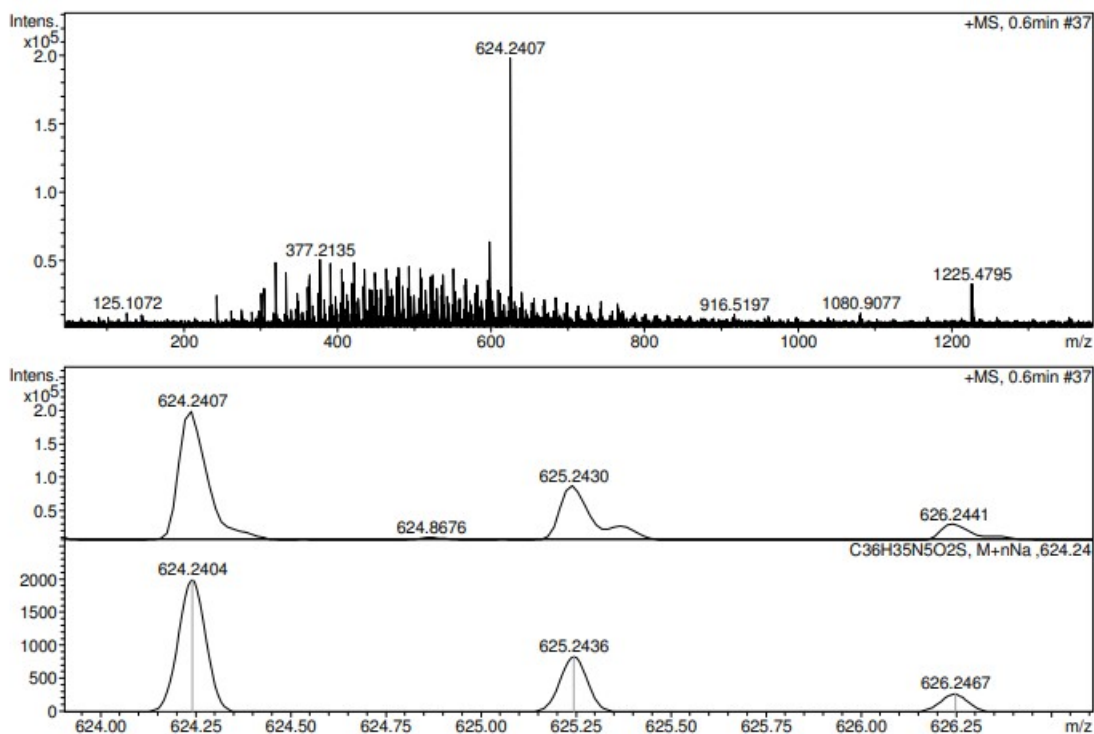


**Fig. S2** ESI HRMS spectrum of **JER** obtained mass = 624.2407 Da, calculated mass = 624.2404 Da

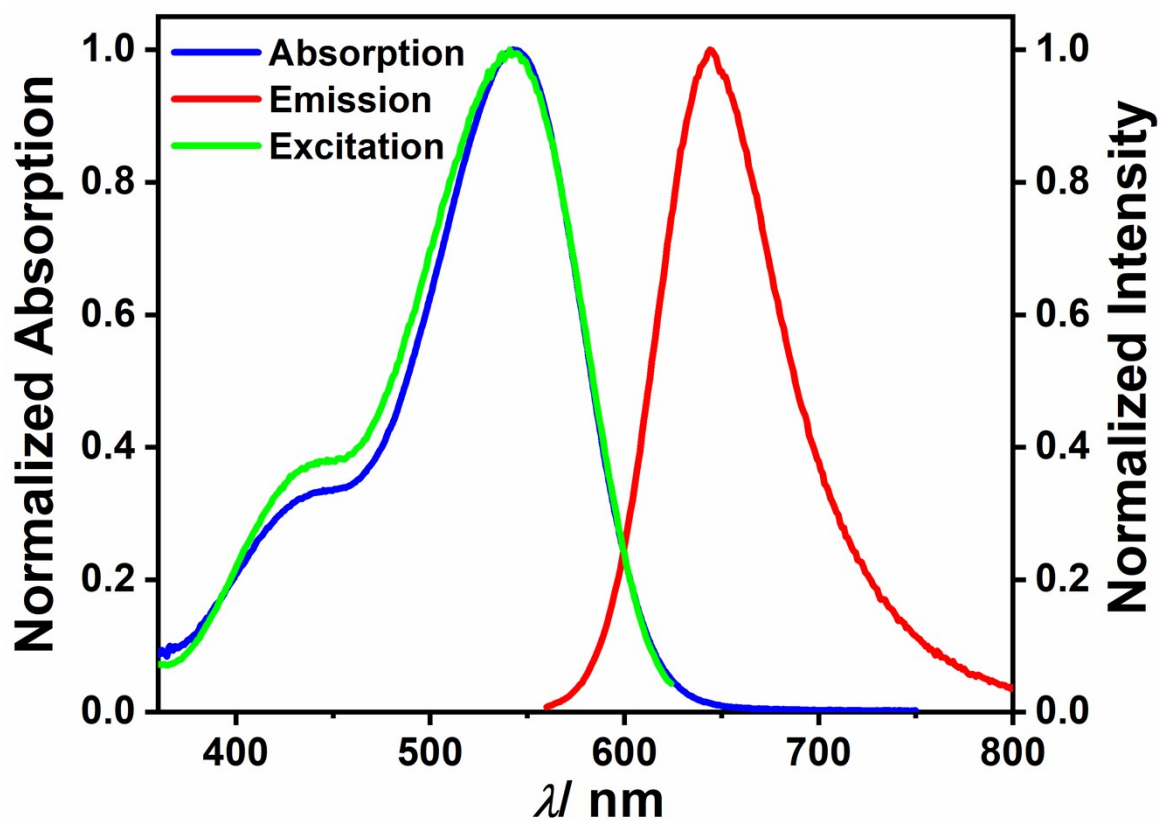


**Fig. S3** Absorption, emission ( $\lambda_{\text{ex}} = 540$  nm) and excitation ( $\lambda_{\text{em}} = 644$  nm) spectra of 5  $\mu\text{M}$  **JER** in DMSO

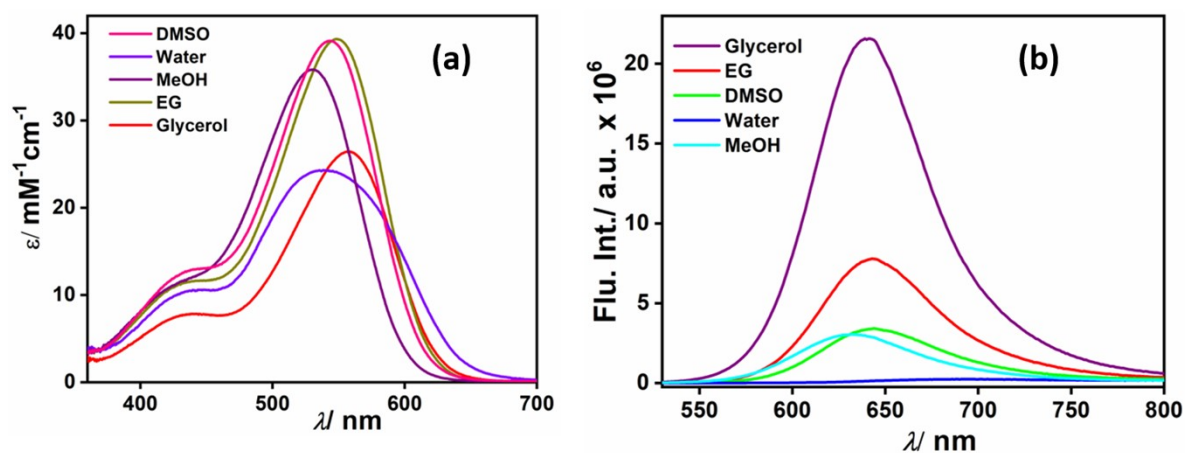


**Fig. S4** Solvent-dependent (a) UV-Vis. absorption spectra and (b) steady state fluorescence emission spectra of 5  $\mu\text{M}$  JER

**Table S1:** Solvent-dependent photophysical parameters of JER

Solvent	$E_T(30)^2$ ( $[\eta]/cP$ )	$\lambda_{max}^{abs.}$ nm	$\lambda_{max}^{em.}$ nm	Stokes shift/ nm	Molar extinction coefficient at $\lambda_{max}^{abs.}$ $M^{-1}cm^{-1}$	Rel. QY (%) <sup>a</sup>
Water	63 (1.0)	539	690	151	24290	0.2
MeOH	55 (0.5)	530	632	102	35820	2.0
DMSO	458 (2.0)	543	644	101	39120	3.0
Ethylene Glycol	53 (18.0)	548	643	95	39340	6.0
Glycerol	57 (905)	557	641	84	26440	31.0

<sup>a</sup> Relative quantum yield is measured using Nile red (QY = 0.7) as a standard (<https://www.photochemcad.com/databases/common-compounds/acridines/nile-red>)

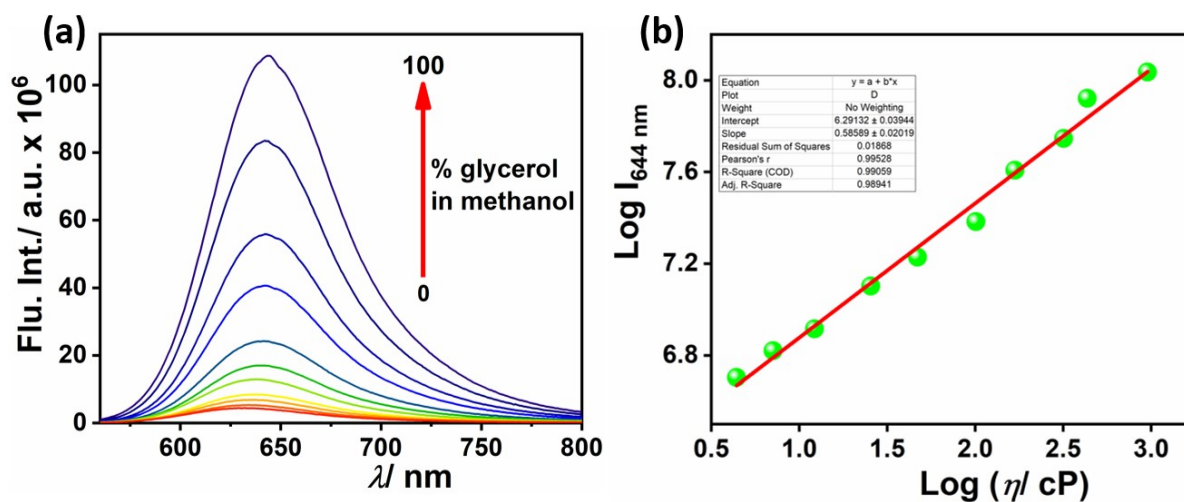


**Fig. S5** (a) Steady state fluorescence emission spectra of 5  $\mu\text{M}$  **JER** in different methanol glycerol mixture (b) double logarithmic plot of fluorescence maxima against the viscosity of the solution fitted linearly

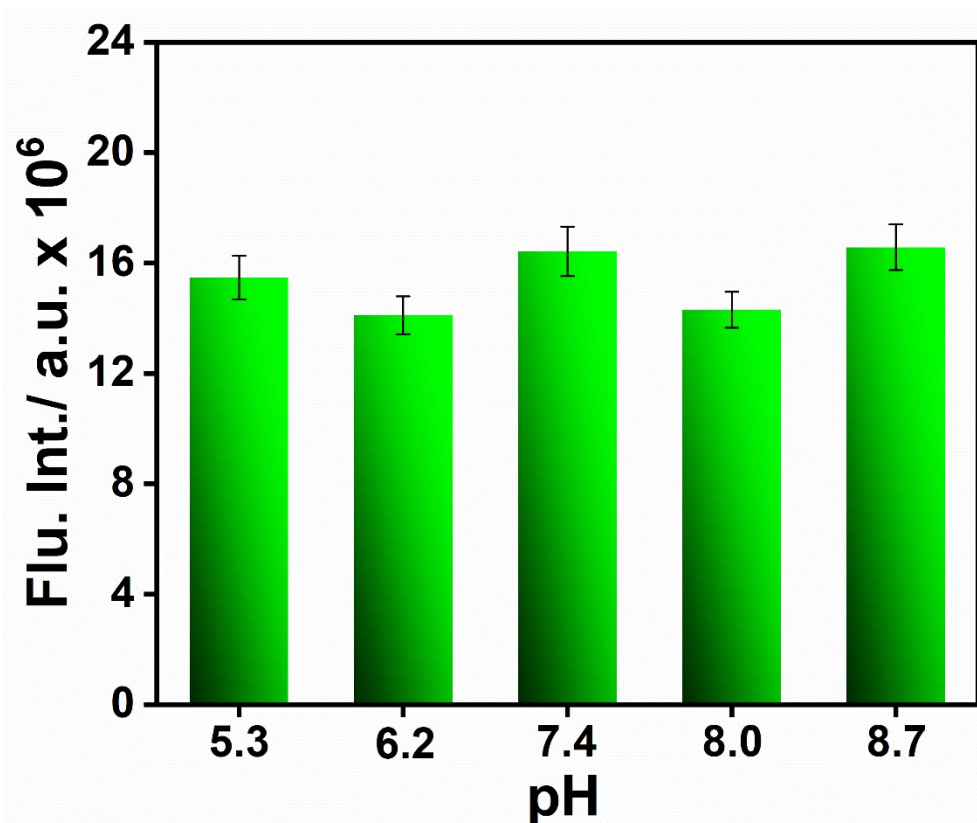


**Fig. S6** Fluorescence emission spectra of **JER** at different pH in 90% glycerol water mixture

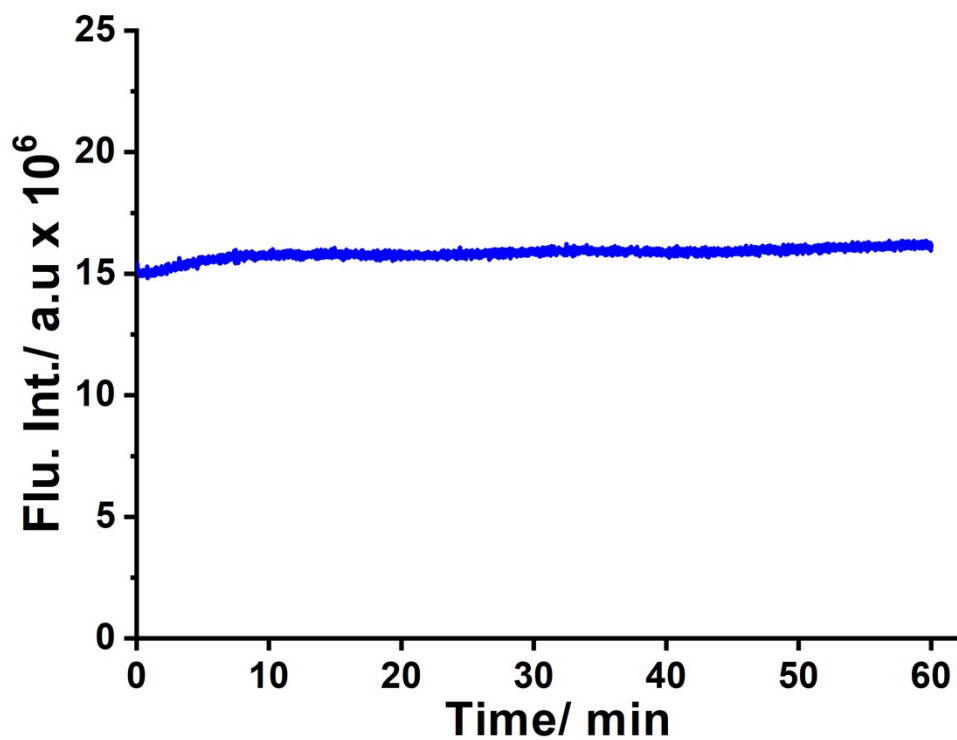


Fig. S7 Plot of fluorescence intensity measured at the emission maxima with time showing photostability of JER under continuous irradiation from 450 W Xenon lamp with 90 lx

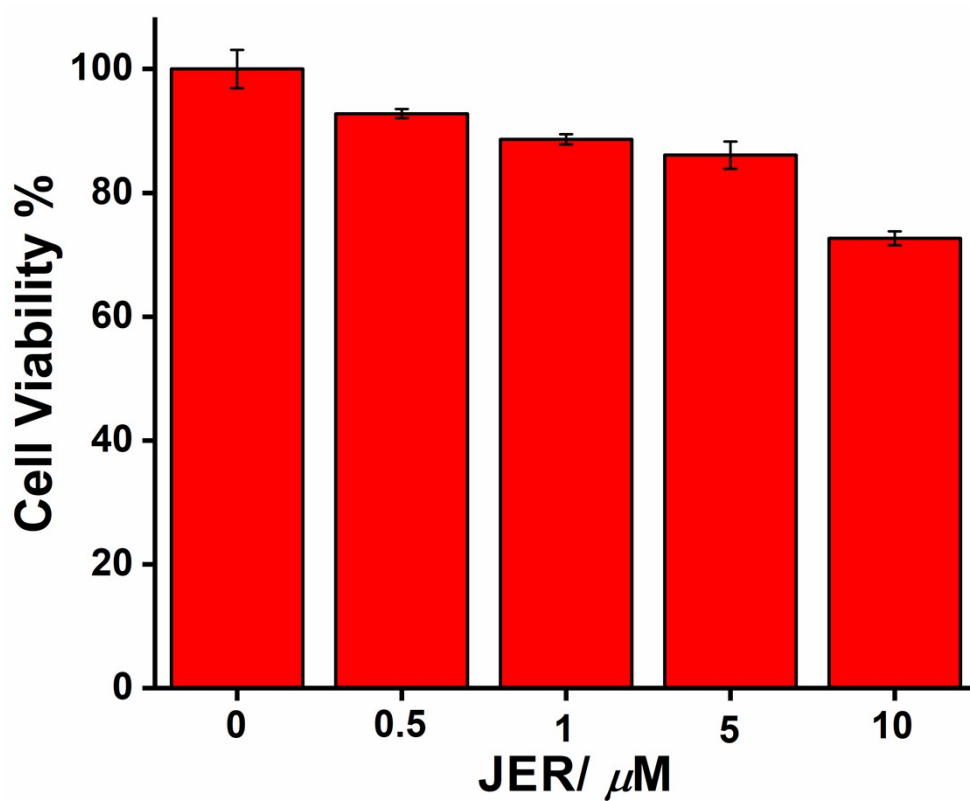
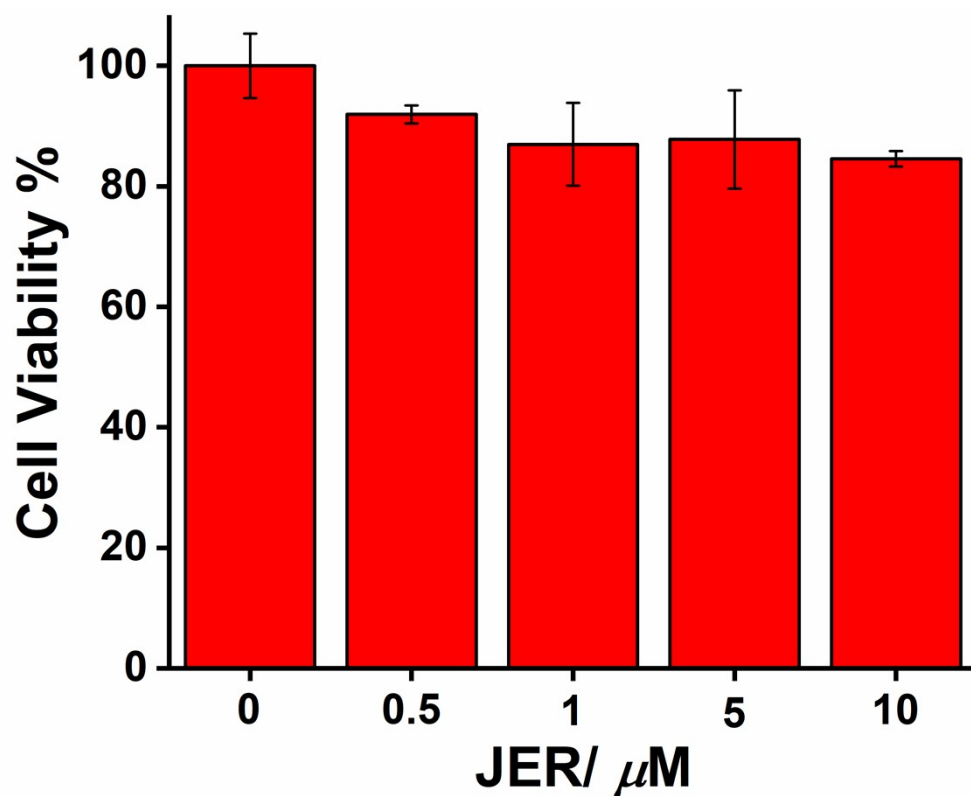
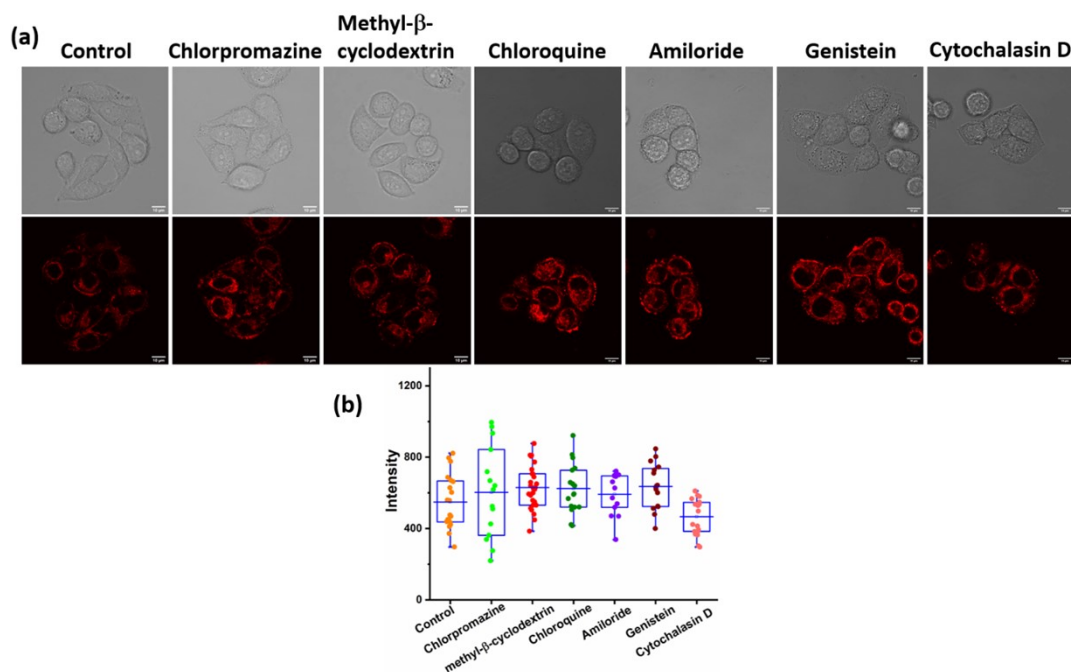


Fig. S8 MTT assay of JER after 24 h incubation with different concentration in A549 cells.





**Fig. S9** MTT assay of **JER** after 24 h incubation with different concentration in HEK 293 cells.



**Fig. S10** (a) Confocal laser scanning microscopy images (CLSM) of HeLa cells treated with indicated endocytosis inhibitors for optimum time point subsequently with structurally similar **JER** derivative ( $0.5 \mu\text{M}$ ,  $\lambda_{\text{ex}} = 561 \text{ nm}$ ,  $\lambda_{\text{em}} = 570\text{-}670 \text{ nm}$ ) for 2 h at  $37 \text{ }^\circ\text{C}$ , (b) quantification of the intensity from the internalized dye to the cells ( $n = 20$  cells).

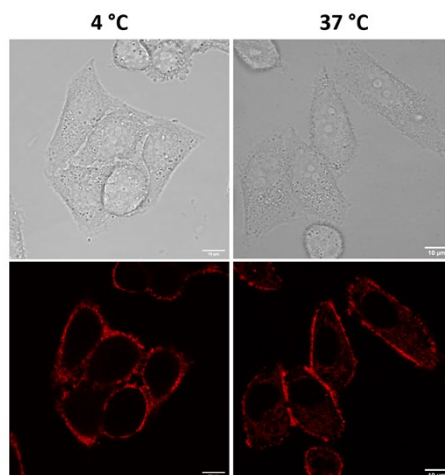


**Fig. S11** Confocal laser scanning microscopy images of HeLa cells incubated with structurally similar **JER** derivative ( $0.5 \mu\text{M}$ ,  $\lambda_{\text{ex}} = 561 \text{ nm}$ ,  $\lambda_{\text{em}} = 570\text{-}670 \text{ nm}$ ) for 15 min at  $4 \text{ }^\circ\text{C}$  and  $37 \text{ }^\circ\text{C}$ . Scale bar =  $10 \mu\text{m}$

**Note:** To understand the possible cellular uptake pathways of a structurally similar **JER** derivative we have utilized several known inhibitors like methyl- $\beta$ -cyclodextrin (clathrin-independent pathway), chlorpromazine (clathrin-mediated endocytosis), Cytochalasin-D (phagocytosis inhibitor through inhibition of actin polymerization), chloroquine (autophagic flux inhibitor), genistein (caveolae-mediated uptake inhibitor), and amiloride hydrochloride (inhibitor of  $\text{Na}^+/\text{K}^+$  exchange) (**Fig. S11**). The internalization of the dye was affected partly by cytochalasin D with 20 % decrease in cellular uptake indicating partly internalization through phagocytosis. We have observed the endocytosis is *energy-dependent* as the internalization of the dye on incubation at  $4 \text{ }^\circ\text{C}$  was quite less as compared to  $37 \text{ }^\circ\text{C}$  (**Fig. S12**). We are further investigating the detailed cellular uptake mechanism and inhibition of metabolic pathways for the energy dependent endocytosis in our follow-up study.

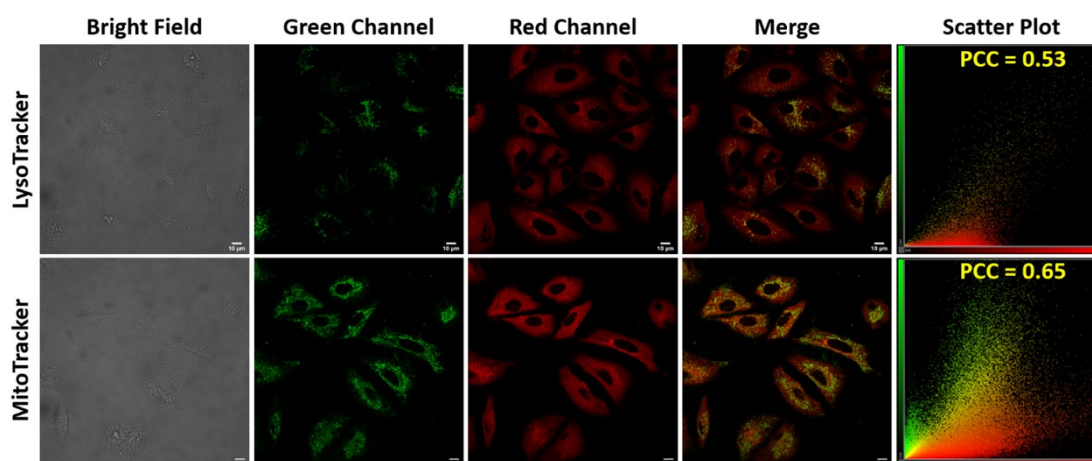


**Fig. S12** Confocal laser scanning microscopy fluorescence images of A549 (lung cancer) cells incubated with  $1 \mu\text{M}$  **JER** and  $0.3 \mu\text{M}$  commercially available trackers for 30 mins. First row representing the colocalization with LysoTracker green and second row for MitoTracker green. Green channel is the fluorescent images from commercially available trackers ( $\lambda_{\text{ex}} = 488 \text{ nm}$ ,  $\lambda_{\text{em}} = 500\text{-}540 \text{ nm}$ ), red channel is the fluorescent images from **JER** ( $\lambda_{\text{ex}} = 560 \text{ nm}$ ,  $\lambda_{\text{em}} = 570\text{-}670 \text{ nm}$ ), fourth column is merge of green and red channel, fifth column is scatter plot with obtained Pearson correlation coefficient. Scale Bar =  $10 \mu\text{m}$

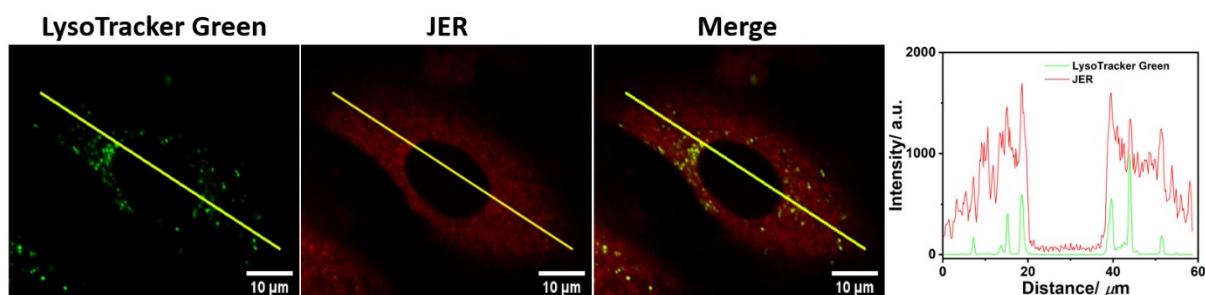


**Fig. S13** Confocal laser scanning microscopy fluorescence images of A549 cells incubated with 1  $\mu\text{M}$  **JER** and 0.3  $\mu\text{M}$  LysoTracker green for 30 mins. Fluorescence from LysoTracker green ( $\lambda_{\text{ex}} = 488$  nm,  $\lambda_{\text{em}} = 500\text{-}540$  nm), **JER** ( $\lambda_{\text{ex}} = 560$  nm,  $\lambda_{\text{em}} = 570\text{-}670$  nm), merge of green and red channel, intensity profile plot of ROI in the image indicating different profile of LysoTracker green and **JER**. Scale bar = 10  $\mu\text{m}$

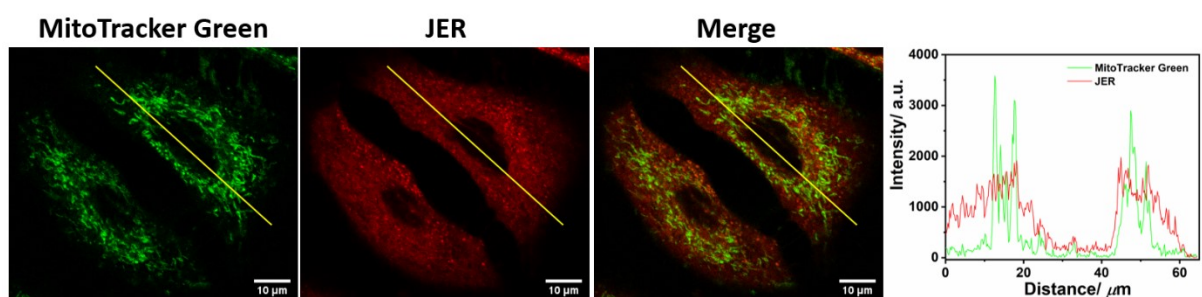


**Fig. S14** Confocal laser scanning microscopy fluorescence images of A549 cells incubated with 1  $\mu\text{M}$  **JER** and 0.3  $\mu\text{M}$  MitoTracker green for 30 mins. Fluorescence from MitoTracker green ( $\lambda_{\text{ex}} = 488$  nm,  $\lambda_{\text{em}} = 500\text{-}540$  nm), **JER** ( $\lambda_{\text{ex}} = 560$  nm,  $\lambda_{\text{em}} = 570\text{-}670$  nm), merge of green and red channel, intensity profile plot of ROI in the image indicating different profile of MitoTracker green and **JER**. Scale bar = 10  $\mu\text{m}$

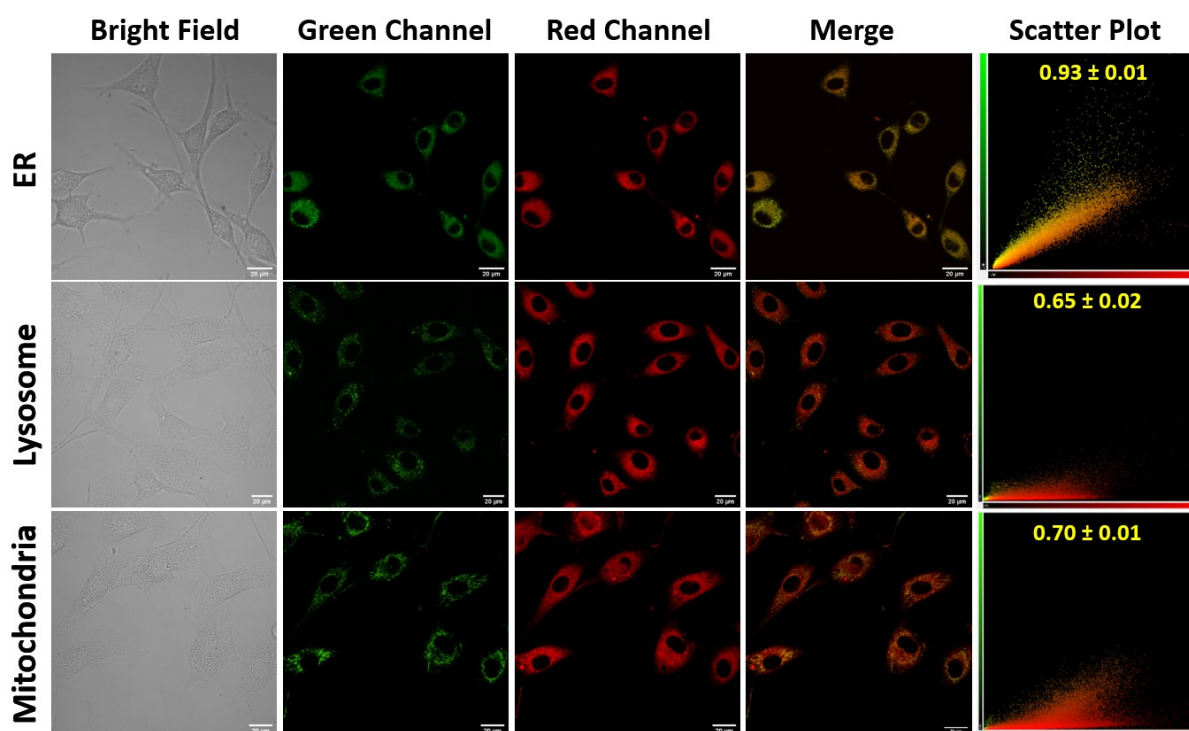


**Fig. S15** Confocal laser scanning microscopy fluorescence images of U-87 MG cells incubated with  $1 \mu\text{M}$  **JER** and  $0.3 \mu\text{M}$  commercially available trackers for 30 mins. First row representing the colocalization with ER Tracker green, second row for LysoTracker green, third row for MitoTracker green. Green channel is the fluorescent images from commercially available trackers ( $\lambda_{\text{ex}} = 488 \text{ nm}$ ,  $\lambda_{\text{em}} = 500\text{-}540 \text{ nm}$ ), red channel is the fluorescent images from **JER** ( $\lambda_{\text{ex}} = 560 \text{ nm}$ ,  $\lambda_{\text{em}} = 570\text{-}670 \text{ nm}$ ), fourth column is merge of green and red channel, fifth column is scatter plot with obtained Pearson correlation coefficient. Scale Bar =  $20 \mu\text{m}$

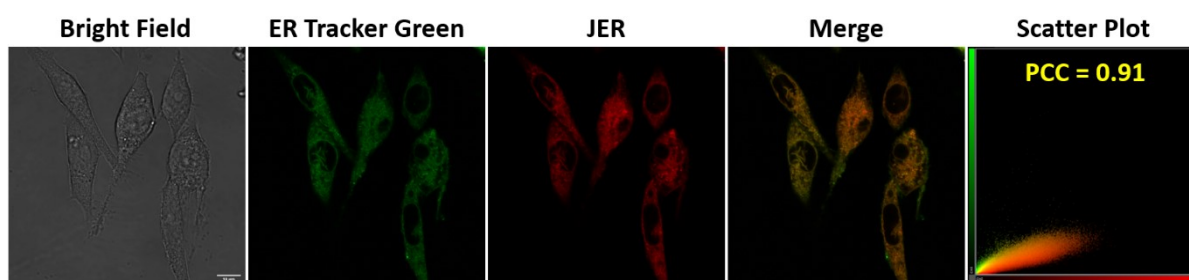


**Fig. S16** Confocal laser scanning microscopy fluorescence images of R1610 cells incubated with  $1 \mu\text{M}$  **JER** and  $0.3 \mu\text{M}$  ER Tracker green for 30 mins. Green channel is the fluorescent images from commercially available trackers ( $\lambda_{\text{ex}} = 488 \text{ nm}$ ,  $\lambda_{\text{em}} = 500\text{-}540 \text{ nm}$ ), red channel is the fluorescent images from **JER** ( $\lambda_{\text{ex}} = 560 \text{ nm}$ ,  $\lambda_{\text{em}} = 570\text{-}670 \text{ nm}$ ), fourth column is merge of green and red channel, fifth column is scatter plot with obtained Pearson correlation coefficient (PCC=0.91). Scale Bar =  $10 \mu\text{m}$

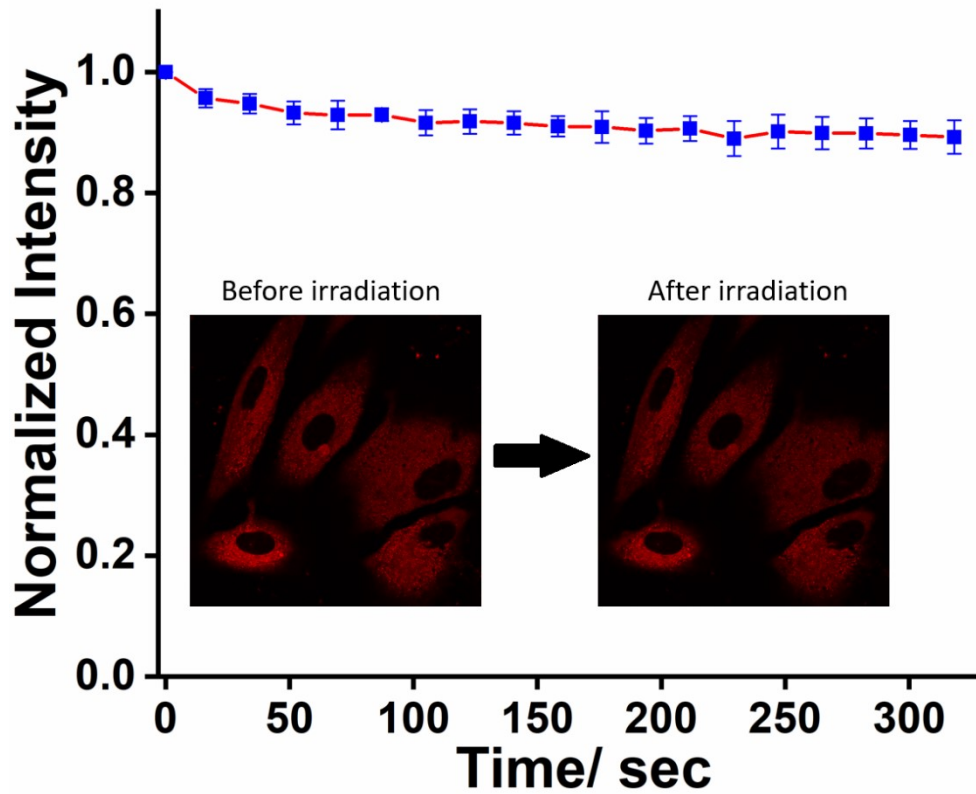


**Fig. S17** Normalized intensity plot of **JER** under live cell conditions with continuous scanning up to 200 scans

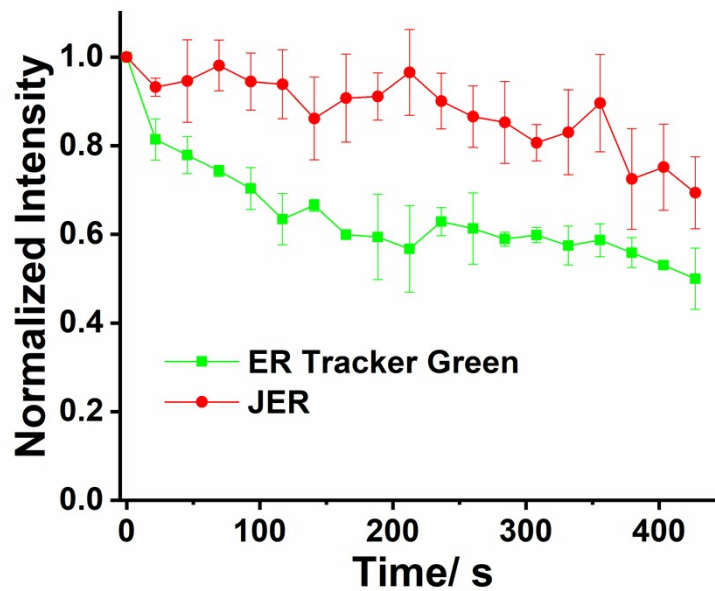


**Fig. S18** Plot of normalized fluorescence intensity of **JER** and ER Tracker Green from cells with continuous imaging condition.

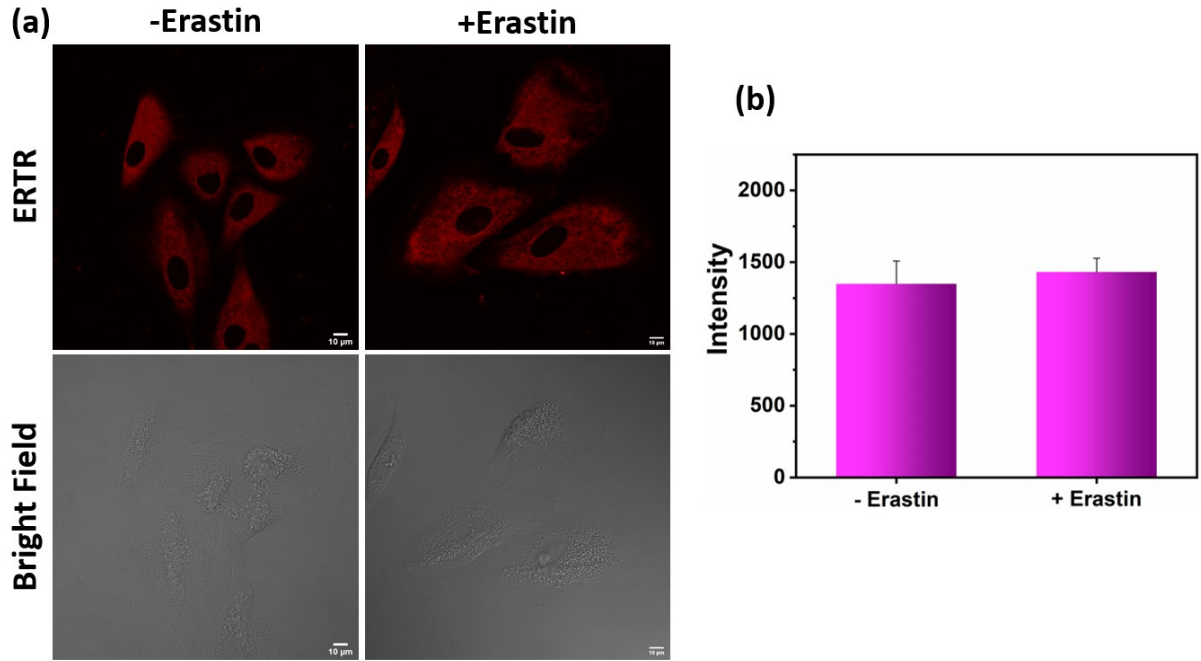


**Fig. S19** Confocal microscopy fluorescence images of the cells pretreated with and without 10  $\mu\text{M}$  erastin for 4 h then stained with 1  $\mu\text{M}$  ER Tracker Red (ERTR) (b) Analysis of quantitative fluorescence intensity in (a) indicating no change in fluorescence intensity. Scale bar = 10  $\mu\text{m}$

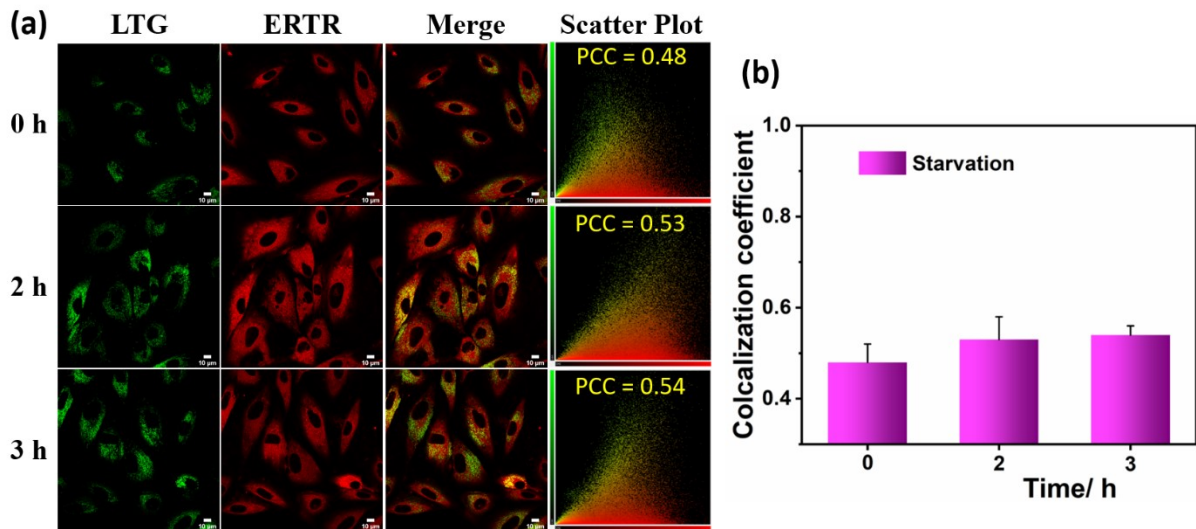


**Fig. S20** (a) Confocal fluorescence microscopy images of the cells co-incubated with 0.3  $\mu\text{M}$  LTG and 1  $\mu\text{M}$  ER Tracker Red (ERTR) for 30 mins and then starved for the indicated time period (b) bar plot of the corresponding Pearson's correlation coefficient. LTG: ( $\lambda_{\text{ex}} = 488 \text{ nm}$ ,  $\lambda_{\text{em}} = 500\text{-}540 \text{ nm}$ ), ERTR: ( $\lambda_{\text{ex}} = 560 \text{ nm}$ ,  $\lambda_{\text{em}} = 570\text{-}670 \text{ nm}$ ). Scale bar = 10  $\mu\text{m}$

**Table S2** Reported viscosity sensitive probes for endoplasmic viscosity

<b>Molecular Rotor</b>	$\lambda_{max}^{abs}/$ <b>nm</b>	$\lambda_{max}^{em}/$ <b>nm</b>	<b>Far-red emission</b>	<b>Detection method</b>	<b>Ferroptosis /ER-phagy</b>	<b>Reference</b>
<b>1</b>	490	516	No	Flu. intensity and Flu. lifetime	No/No	<i>Chem. Commun.</i> , 2014, <b>50</b> , 11672-11675
<b>1</b>	490	515	No	Flu. intensity and Flu. lifetime	Reticulo-phagy	<i>Chem. Commun.</i> , 2019, <b>55</b> , 2453-2456
<b>GE-Y</b>	430	550	No	Flu. intensity	No/No	<i>Chem. Commun.</i> , 2022, <b>58</b> , 10727-10730
<b>Ir-ER</b>	405/ 810 (two photon)	530	No	Flu. lifetime	Yes/No	<i>Chem. Commun.</i> , 2021, <b>57</b> , 5040-5042
<b>1b</b>	550	648	Yes	Flu. intensity	No/No	<i>J. Mater. Chem. B</i> , 2021, <b>9</b> , 5664-5669
<b>PV1</b>	481	616	Yes	Flu. intensity	Yes/No	<i>Anal. Chim. Acta</i> , 2022, <b>1232</b> , 340454
<b>DSPI-3</b>	560	620	Yes	Flu. intensity	Yes/No	<i>Anal. Chem.</i> , 2022, <b>94</b> , 6557-6565
<b>JER</b>	540	645	Yes	Flu. intensity and Flu. lifetime	Yes/Yes	<b>This work</b>

**References:**

1. A. Silswal, A. Kanojiya and A. L. Koner, *Front. Chem.*, 2022, **10**, 10.3389/fchem.2022.840297.
2. In *Solvents and Solvent Effects in Organic Chemistry*, 2010, DOI: <https://doi.org/10.1002/9783527632220.ch7>, pp. 425-508.